Distribution Grid Stability—Influence of Inertia Moment of Synchronous Machines

Tomáš Petrík, Milan Daneček, Ivan Uhlíř, Vladislav Poulek and Martin Libra *

Department of Physics, Faculty of Engineering, Czech University of Life Sciences Prague, Kamýcká 129, 16500 Prague, Czech Republic; tom.petr11@seznam.cz (T.P.); milan.danecek@gmail.com (M.D.); uhliri@tf.czu.cz (I.U.); poulek@tf.czu.cz (V.P.)

* Correspondence: libra@tf.czu.cz

Abstract: This paper shows the influence of grid frequency oscillations on synchronous machines coupled to masses with large moments of inertia and solves the maximum permissible value of a moment of inertia on the shaft of a synchronous machine in respect to the oscillation of grid frequency. Grid frequency variation causes a load angle to swing on the synchronous machines connected to the grid. This effect is particularly significant in microgrids. This article does not consider the effects of other components of the system, such as the effects of frequency, voltage, and power regulators.

Keywords: angle swinging; grid frequency oscillations; electromechanical system; inertial masses; microgrids

1. Introduction

The idea of grid voltage having a coherent sinusoidal course with constant frequency does not correspond with the reality of phenomena occurring in the distribution grid. Accurate measurements disclose oscillations of grid frequency and an instantaneous phase of distribution grid voltage. Grid frequency oscillation has a random noise trend because it is only the response of an energy system to a casually changing daily demand energy diagram [1]. This effect is particularly significant in microgrids [2–4]. The issue of network stability has been studied in a number of other works (e.g., [5]).

The phenomenon of grid oscillations may be described in terms of statistical dynamics using the power spectral density $S_\omega(\Omega)$ of a distribution grid's angular frequency fluctuation. An example of this function characterizing the frequency spectrum of grid frequency deviations is shown in Figure 1.

A spectrum of grid frequency deviations has two components: (i) A slow component for $\Omega < 2s^{-1}$ (mean $\Delta F < 0.32$ Hz), which is determined by the properties of rotational regulation in power plants as well as the properties of superior central frequency regulation. The interconnection of originally regional districts of the distribution grid into larger complex grids and, later, into the European central grid caused a reduction in the amplitude of very slow fluctuations. Then, this phenomenon continued, leading to the current state of zero steady-state error in the distribution grid frequency. (ii) A fast component for $\Omega > 2s^{-1}$ (mean $\Delta F > 0.32$ Hz), which is determined by an angular elasticity of the supply system in the case of power changes. A fast component originates from the magnitude and phase changes of instant voltage as it decreases on a power line, and the resulting fast load changes cause transformer impedances in the distribution grid. The angular elasticity refers to the angular elasticity of the phasors of voltage.

Figure 1 shows some samples of the spectrograms of fluctuation in the angular frequency of the distribution grid. Modern distribution grids with digital control of frequency have zero difference on average from central frequency, but there are visible fluctuations of frequency and phasor angle in an area up to $\Omega > 2$ s^{-1} (mean $\Delta F > 0.32$ Hz).

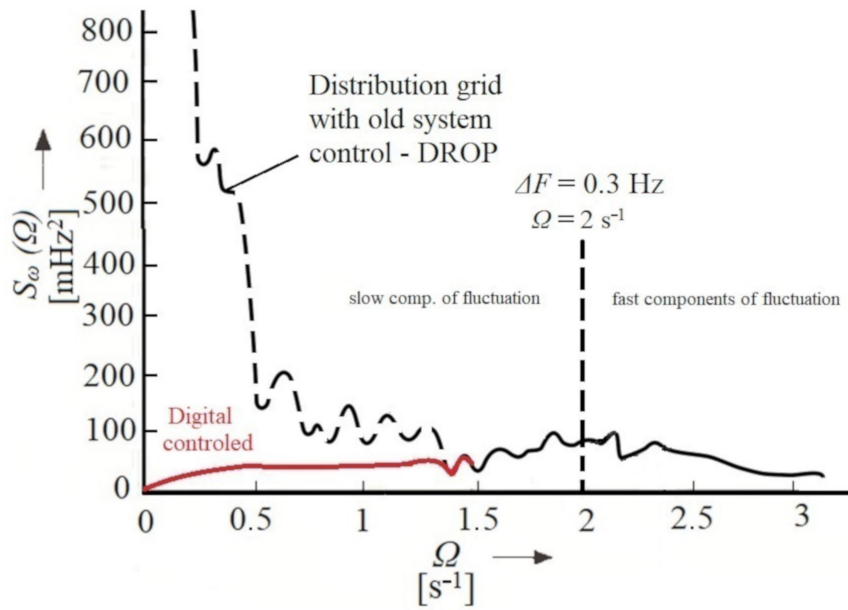**Figure 1.** Examples of power spectral density $S\omega(\Omega)$ at frequency fluctuation Ω.

If a synchronous machine driving inertial masses is connected to the grid, the mechanical movement of a machine shaft must follow frequency and phase changes of a voltage phasor of the grid. A shaft follows the instantaneous grid voltage phase with an angle deviation, producing a load angle β in a synchronous machine. The instantaneous power consumed or supplied by a machine to a grid depends on the magnitude and orientation of the load angle β. The greater the inertial masses on the shaft are in comparison to the size of a synchronous machine, the greater the dynamic deviation of the following fast grid phase changes and load angle oscillations will be [6].

Since an electromechanical system (a synchronous machine and its inertial masses) has very low oscillation dumps, the load angles, excited by distribution grid frequency fluctuations, have a harmonic swinging character. In addition, they are accompanied by an undesirable overflow of energy between the grid and the inertial masses on the shaft.

2. Description of a Modeled System

The electromechanical swinging system consists of the rigidity of a synchronous machine magnetic field, the damping effects, and the moment of inertia, which are connected with a shaft as presented in Figure 2. The system in Figure 2 is described by the differential equation

$$I\ddot{\beta} + B\dot{\beta} + k\beta = \frac{I}{P_d}\dot{\omega},\tag{1}$$

where β is the load angle of a synchronous machine, ω is the grid frequency (s^{-1}), I is the overall moment of inertia connected to a shaft $(kg \cdot m^2)$, B is the torsion damping constant $(N \cdot m \cdot s)$, K is the torsion rigidity of a synchronous machine $(N \cdot m)$, and P_d is the number of pole pairs in a synchronous machine.
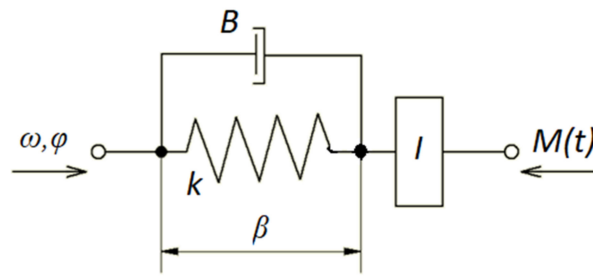
Figure 2. Electromechanical vibrating set of a synchronous machine.

For simplification, the following will be assumed:

- An unloaded synchronous machine;
- Linearity of the magnetic circuit;
- The exclusion of the influence of external voltage, power, and frequency control circuits;
- The possession of torque characteristics for small $|\beta|$ (< 0.1 rad) in linearized solutions.

The precision of the system is described by Equation (1) in Laplace's transformation [7,8]:

$$G(p) = \frac{pI}{P_d\,(p^2I + pB + k)}.$$ (2)

The power spectral density of the load angle fluctuation is

$$S_\beta(\Omega) = \lim_{n \to \infty} (G(p))^2\, S_\omega(\Omega),$$ (3)

where $S_\beta(\Omega)$ is the power spectral density of the load angle fluctuation and $S_\omega(\Omega)$ is the power spectral density of fluctuation for angular frequency fluctuations (s^{-2}).

$$S_\beta(\Omega) = \frac{\Omega^2 I^2 S_\omega(\Omega)}{P_d\left[(k - \Omega^2 I)^2 + \Omega^2 B^2\right]}.$$ (4)

The natural frequency of the system is Ω_0:

$$\Omega_0 = \sqrt{\frac{k}{I}}.$$ (5)

The coefficient of a relative system damping

$$a = \frac{B}{2\sqrt{kI}}$$ (6)

is very low for most synchronous machines; it is usually < 0.1, in which case the resonance is very selective. The system transmits just the natural frequency. A system response has almost a sinusoidal course of load density swinging with an amplitude β_A. From Equation (4), the results for $\Omega = \Omega_0$ can be written as

$$S_\beta(\Omega_0) = \beta_A^2 = \frac{I^2}{P_d^2\,B^2} = S_\omega(\Omega_0).$$ (7)

3. Maximum Admissible Grid Frequency Oscillations

If the response of a load angle's swing has to have an amplitude A as the maximum, the power spectral density $S_\omega(\Omega_0)$ of the grid angle frequency must not be greater than $S_{\omega,max}(\Omega_0)$

$$S_{\omega,max}(\Omega_0) = \frac{P_d^2 B^2}{I^2} \beta_A^2, \tag{8}$$

where $S_{\omega,max}(\Omega_0)$ is the upper limit of the power spectral density of a grid angle frequency (s^{-2}).

Substituting the variable Ω_0 from Equation (5) into Equation (8) for the parameter I yields

$$S_{\omega,max}(\Omega_0) = \frac{P_d^2 B^2}{k^2} \beta_A^2 \, \Omega_0^4. \tag{9}$$

The maximum size of a flying wheel for which the amplitude of the load angle's swing does not exceed the given value β_A is thus determined.

Courses for $S_{\omega,max}(\Omega_0)$ according to Equation (9) for the chosen β_A (e.g., 0.1, 0.15, and 0.2 rad) are drawn in Figure 3. These courses constitute the upper limits of power spectral density in the grid angle frequency fluctuations $S_{\omega,max}(\Omega_0)$ for the permitted β_A. The courses of the upper limits are fitted with a scaled I according to Equation (5):
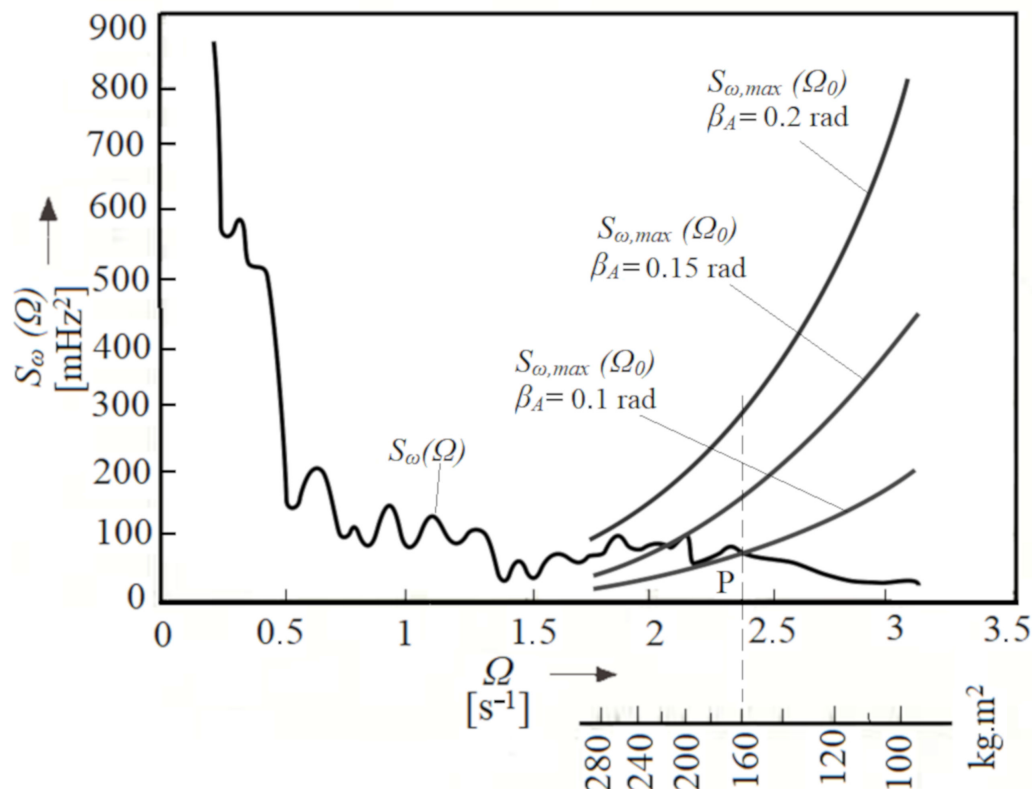
$$I = \frac{k}{\Omega_0^2} \tag{10}$$

Figure 3. Influence of the fluctuation spectrum of the grid and inertial momentum I on the amplitude of angular oscillation.

The maximum value of the moment of inertia being placed on the shaft of a synchronous machine is given by the first intersection point (from the right) of the function $S_{\omega,max}(\Omega_0)$ for the permissible

maximum of the load angle oscillation amplitude β_A with the course $S_\omega(\Omega)$ measured in the grid section at the considered time.

4. Practical Verifying

The synchronous machine MEZ-A 225 MO 4 with the parameters P_s = 50 kVA, n = 1500 min^{-1}, k = 1140 N·m, and B = 14 N·m·s was chosen as an example. MEZ-A 225 MO 4 is a synchronous hydroalternator with four poles, without a dumper, with a brushless exciter powered by an external electronic source with a constant current of 1.2 A. This corresponds to excitation at a nominal voltage of 3 × 400 V in the idle state.

This excitation current of the brushless exciter was kept constant throughout the experiment.

The shaft of the machine was connected by a rigid coupling with a steel flywheel with a diameter of 1300 mm mounted in its own bearings.

The moment of inertia I = 160 kg·m^2 was determined by calculation from the geometric dimensions and the catalog data. The damping constant B = 14 N·m·s was calculated from the attenuation of the transient during phasing into the distribution network.

The unit was started at synchronous velocity by using a friction coupling from a diesel engine.

During the experiment, the synchronous machine ran as a motor on the distribution network without any additional load. It was loaded by mechanical losses in the bearings and the mechanical power consumption of its own ventilation and exciter. The total load was estimated at 3 kW, which is less than 8% of the nominal power of the synchronous machine. This state was close to the idling state, which is theoretically discussed above.

Under the permissible load angle oscillation amplitude β_A = 0.1 rad (equal to the overflow of active power P_a = 20 kW), the intersection point P presented the maximum value I = 160 kg·m^2.

Figure 4 gives evidence of conformity to the calculated value of an average amplitude (I = 160 kg·m^2) with a recording of grid frequency fluctuation and the corresponding response of the load angle. This recording was measured from the machine during the experiment.
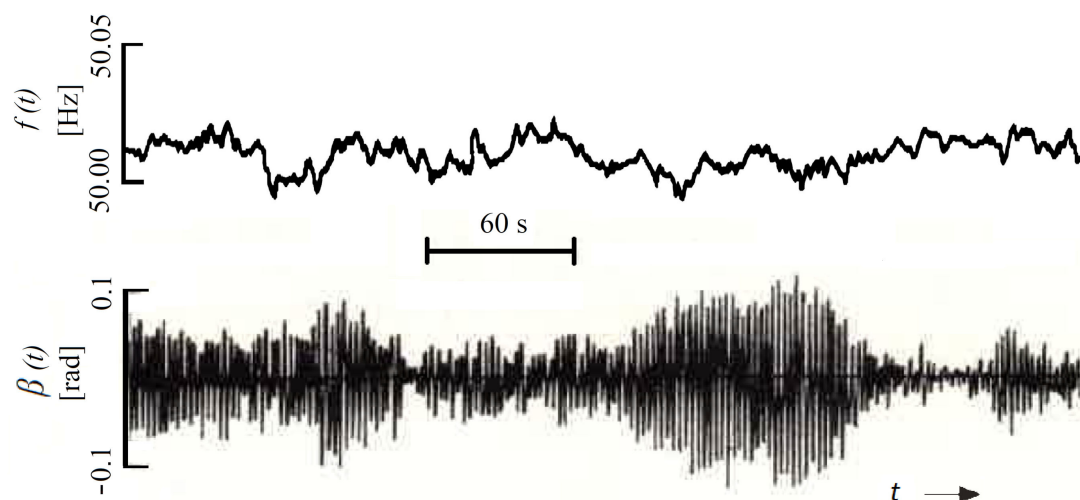

Figure 4. Random changes in grid frequency (top) and changes influenced by the oscillation of the load angle of a synchronous machine (bottom).

5. Conclusions

Grid frequency variation causes a load angle to swing in the synchronous machines connected to the grid. The grid frequency variation spectrum shape grows the inertial moment on the shaft of the synchronous machine while also growing the swinging amplitude. This is visible from the shown equations. The maximum inertia moment value was thus determined for safe swinging amplitude. The evidence of conformity to the calculated value of the moment of inertia is shown in Figure 4 as a

recording of grid frequency and the corresponding response of the load angle. The average value of the load angle is present in the required interval. The instantaneous value of the load angle is mainly present in the required interval; however, the average value is more significant.

The load angle in this safe interval enables the machine to be driven in a safe and reliable manner by external controllers. These controllers are not considered in the article. This limitation should be respected both in drives with tens and hundreds of kW as well as in drives with small synchronous machines and stepping motors, where large inertial masses have to be driven.

As was written before, this paper did not consider external controllers. However, they are often a major part of frequency grid stability issues. Frequency grid fluctuations cause load angle fluctuations, which in turn cause frequency grid fluctuations. This interaction is a closed circle. In closing, it is necessary to mention trends and possibilities in frequency stabilization. A few studies last year discussed renewable sources of energy. These renewable sources can reduce the quality of grid services [9]. However, with the appropriate combination, along with batteries, they can be used to stabilize the properties of the grid [9]. A small battery source connected to photovoltaic panels was described in [10]. These battery sources, or even larger ones, would therefore be appropriate to include and use in the grid. This is especially true for intelligent buildings that combine many energy sources such as synchronous generators and photovoltaic panels; these batteries can be used as more than just backup sources.

Author Contributions: Conceptualization, T.P., I.U.; investigation, T.P., I.U., M.L.; methodology, M.D., V.P.; supervision, M.L.; validation, V.P., M.D.; visualization, V.P., M.L.; writing—original draft, I.U., T.P.; writing—review and editing, T.P., M.L. All authors have read and agreed to the published version of the manuscript.

Nomenclature

$S_\omega(\Omega)$	power spectral density of distribution grid's angular frequency fluctuation
Ω	angular frequency of fluctuations
B	load angle of a synchronous machine
ω	grid frequency
I	overall moment of inertia connected to a shaft
B	torsion damping constant
K	torsion rigidity of a synchronous machine (N·m)
P_d	number of pole pairs of a synchronous machine
Ω_0	natural frequency of the system
S_β	(Ω) power spectral density of the load angle fluctuation β_A
β_A	load angle of a synchronous machine at the natural frequency of the system
a	coefficient of a relative system damping
$S_{\omega,max}$	(Ω_0) upper limit of the power spectral density of a grid angle frequency
P_s	power of a unit used for experimentation
n	nominal revolutions of a unit
P_a	active power

References

1. Amin, W.T.; Montoya, O.D.; Garrido, V.M.; Gil-González, W.; Garces, A. Voltage and Frequency Regulation on Isolated AC Three-phase Microgrids via s-DERs. In Proceeding of the 2019 IEEE Green Technologies Conference (GreenTech), Lafayette, LA, USA, 3–6 April 2019; pp. 1–6.
2. Ferro, G.; Robba, M.; Sacile, R. A Model Predictive Control Strategy for Distribution Grids: Voltage and Frequency Regulation for Islanded Mode Operation. *Energies* **2020**, *13*, 2637. [CrossRef]

3.　Delfino, F.; Ferro, G.; Robba, M.; Rossi, M. An architecture for the optimal control of tertiary and secondary levels in small-size islanded microgrids. *Int. J. Electr. Power Energy Syst.* **2018**, *103*, 75–88. [CrossRef]

4.　Delfino, F.; Rossi, M.; Ferro, G.; Minciardi, R.; Robba, M. MPC-based tertiary and secondary optimal control in islanded microgrids. In Proceedings of the 2015 IEEE International Symposium on Systems Engineering (ISSE), Rome, Italy, 28–30 September 2015; pp. 23–28.

5.　Wu, Y.-K.; Tang, K.-T.; Lin, Z.K.; Tan, W.-S. Flexible Power System Defense Strategies in an Isolated Microgrid System with High Renewable Power Generation. *Appl. Sci.* **2020**, *10*, 3184. [CrossRef]

6.　Serra, F.M.; Fernandez, M.L.; Montoya, O.D.; Gil-Gonzalez, W.J.; Hernandez, J.C. Nonlinear Voltage Control for Three-Phase DC-AC Converters in Hybrid Systems: An Application of the PI-PBC Method. *Electronics* **2020**, *9*, 847. [CrossRef]

7.　Han, J.; Liu, Z.; Liang, N.; Song, Q.; Li, P. An Autonomous Power Frequency Control Strategy Based on Load Virtual Synchronous Generator. *Processes* **2020**, *8*, 433. [CrossRef]

8.　Haque, M.E.; Negnevitsky, M.; Muttaqi, K.M. A Novel Control Strategy for a Variable Speed Wind Turbine with a Permanent-Magnet Synchronous Generator. *IEEE Trans. Ind. Appl.* **2010**, *46*, 331–339. [CrossRef]

9.　Yoo, Y.; Jung, S.; Kang, S.; Song, S.; Lee, J.; Han, C.; Jang, G. Dispatchable Substation for Operation and Control of Renewable Energy Resources. *Appl. Sci.* **2020**, *10*, 7938. [CrossRef]

10.　Poulek, V.; Dang, M.Q.; Libra, M.; Beránek, V.; Šafránková, J. PV Panel with Integrated Lithium Accumulators for BAPV Applications—One Year Thermal Evaluation. *IEEE J. Photovolt.* **2020**, *10*, 150–152, ISSN 2156-3403. [CrossRef]